

# SOLVING STRUCTURAL VIBRATION PROBLEMS USING OPERATING DEFLECTION SHAPE AND FINITE ELEMENT ANALYSIS

by

**Maki M. Onari**

**Manager of Turbomachinery Testing**

and

**Paul A. Boyadjis**

**Manager of Turbomachinery Analysis**

**Mechanical Solutions, Inc.**

**Whippany, New Jersey**



*Maki M. Onari is Manager of Turbomachinery Testing at Mechanical Solutions, Inc. (MSI), in Whippany, New Jersey. He is responsible for field vibration testing involving ODS and modal analysis. His career spans more than 12 years, primarily working with rotating equipment analysis and troubleshooting in the petrochemical, refinery, and power generation industries. Prior to joining MSI, Mr. Onari*

*was a Rotating Equipment Engineer in PDVSA-Venezuela, responsible for the predictive maintenance of one of the largest petrochemical complexes in Latin America.*

*Mr. Onari received his B.S. degree (Mechanical Engineering, 1996) from the Zulia University in Venezuela. He is a member of ASME and the ISO TC108/S2 Standards Committee for Machinery Vibration.*



*Paul A. Boyadjis is Manager of Turbomachinery Analysis at Mechanical Solutions, Inc. (MSI), in Whippany, New Jersey. He has nearly 25 years of diverse experience in the analysis and design of rotating equipment. His specialty includes complex 3D solids modeling of pump and compressor casings and rotating assemblies, and the performance of stress and vibration analysis using advanced*

*finite element techniques. Mr. Boyadjis has worked as a lead analytical engineer for major compressor and pump manufacturers such as Ingersoll-Rand, Ingersoll-Dresser Pump, and Flowserve Corporation.*

*Mr. Boyadjis has B.S. and M.S. degrees (Mechanical Engineering) from Lehigh University. He is a member of the API Machinery Standards Committee and a Standards Partner of the Hydraulic Institute.*

geometry change such as looseness or cracking, it becomes more complicated. The trial and error approach can be time consuming and is considered the least cost effective method to solve this type of problem. Therefore, thorough vibration testing combined with detailed calibrated finite element analysis (FEA) models have become powerful tools to identify and mitigate vibration issues through well-conceived fixes while reducing the risk of introducing new ones. This tutorial will provide an in-depth look at how the combination of field testing and computer analysis can solve vibration issues in a timely and cost-effective manner. Several case studies will be presented that demonstrate this method.

## INTRODUCTION

Typically pump original equipment manufacturers (OEMs) and the end users have used vibration information to diagnose and find the root cause of any vibration-related problem by taking a few readings from the bearing housings and sometimes from the shaft (displacement) both during steady and transient conditions of the pump. Approximately 90 percent of the cases of excessive vibration can be diagnosed using such traditional readings from the bearing housings, and the solution can be implemented immediately (e.g., rotor imbalance, misalignment, bearing damage, etc.). However, the remaining 10 percent of pump vibration problems can be more subtle and lead to chronic reliability issues such as premature wear of bushings and seals, bearing failures, structural cracks and looseness, coupling failures, and even broken shafts. One of the more common of these difficult chronic problems is the synchronous excitation of structural natural frequencies, but unexpected problems can also occur due to subsynchronous and supersynchronous problems. These result from rubs, fluid dynamic instabilities, or resonances with high order excitation sources such as vane pass frequency.

Identifying the source of the problem requires a troubleshooting investigation that plant personnel can carry out if they are experienced. Alternatively they can be given appropriate guidance by the OEM or a qualified consultant that uses modern tools and approaches (available from large end user in-house groups, major OEMs, and qualified consulting companies), such as vibration data acquisition analyzers and computer simulation analysis software. The cost associated with this testing and analysis is considered negligible when compared to the expenditures for the continued rebuilding of damaged machinery components and associated downtime. Specifically, these tools include vibration versus time (wave forms), orbit plots, vibration versus time trending, and vibration versus frequency analysis (i.e., a fast Fourier transform [FFT] spectrum). In addition, higher level analysis exists such as operating deflection shapes (ODS), experimental modal analysis (EMA) or “bump” testing, combined with finite element analysis (FEA).

## ABSTRACT

This tutorial focuses on vibration issues in pumps primarily for power plants, refineries, and municipal water and waste water treatment plants. Over the years, the original equipment manufacturer (OEM) and the end user often have been able to solve vibration problems for this kind of equipment based on their experience. An adequate maintenance program can identify and solve typical vibration responses at 1× and 2× running speed due to imbalance or misalignment. However, when the vibration is due to a resonance of a structural natural frequency or an unexpected

## BACKGROUND ON VIBRATION MEASUREMENTS

Excessive vibration of rotating equipment is one of the most common issues that personnel experience industry-wide, from large power plants and refineries to small wastewater treatment plants. In most of the cases, high vibration is a detrimental condition that can lead to wasted energy due to wear of internal seals, environmental harm or physical danger due to failure of exterior seals, undesirable noise, and potential failure of the machine. On the beneficial side, the amplitude of vibration at key frequencies in rotating machinery can be used to characterize how healthy the equipment is, aided by specialized instrumentation. This section of the tutorial will explain the fundamentals of vibration theory and vibration measurement.

### *Vibration Theory*

The fundamental concept of vibration is basically the oscillatory motion of the mass and the forces involved in the system. In general, any mass with elasticity is capable of vibrating. The vibration can be classified in two types, free vibration and forced vibration. The first one occurs when the system oscillates freely after some previous excitation, and the second one occurs when current external forces excite the system. If the frequency of the external force coincides with the natural frequency of the system, a resonance condition will take place making the system vibrate with elevated amplitude. This should be avoided during the design of any structure and especially rotating machinery. Fortunately, if there is a resonance then damping in the system limits the amplitude at the resonance condition to some degree as energy is dissipated by friction and fluid-structure interaction.

### *Vibration Measurement Hardware*

When performing vibration testing (whether routine or for troubleshooting), the instrumentation required depends on the application, location, and purpose. For instance, eddy current proximity probes are used to measure the shaft vibration in displacement relative to the bearing housing in mils or  $\mu\text{m}$ . Velocity sensors are used to measure vibration in velocity in/s or mm/s. To measure vibration on the bearing housings and casings the typical transducers used are piezoelectric accelerometers, which measure the absolute vibration in g's. Modern accelerometers have been designed to measure not only high frequency response, but also have been designed to measure low frequency vibration (down to 1 Hz and in special cases below 1 Hz). However, care must be taken when the vibration in acceleration is integrated to obtain the vibration in terms of velocity or displacement because each vibration peak is divided by its frequency, which could lead into an "integration error" for low frequency spikes, in which a small amount of low frequency noise appears to be a large amount of fictitious displacement. Therefore, the fact that the accelerometers are suitable only for high frequency vibration is no longer true. They are capable of covering a large frequency bandwidth, typically up to 10 kHz or higher, enabled by the typical resonant frequency of the accelerometers being on the order of 50 kHz. Proximity probes do not require integration since they measure relative displacement directly. Hence, they are free of integration error at low frequencies, and at the upper end typically are considered adequate up to several kHz, which is sufficient for pump applications.

Probes that measure velocity directly are also available. However, the construction of these probes results in a relatively limited frequency range, and today accelerometers are typically preferred, even though a degree of integration error will be present at lower frequencies.

Proximity probes are thread mounted through the bearing housing cap or on a bracket next to the housing. These sensors are powered through a "proximitor" box that also converts the direct current (DC) output voltage into displacement. Accelerometers are usually

magnetic mounted for temporary use and also could be thread mounted on the casing with the appropriate stud. They always should be electrically isolated to avoid grounding issues between the pump casing and the analyzer. For temporary use for nonmagnetic surfaces (concrete, plastic, aluminum, austenitic steels, etc.) the accelerometers can be placed with appropriate wax material for low temperature applications, and with epoxy for moderate temperature applications. Hand-held attachment can produce good results if performed by a properly experienced technician and taken at the same location on the equipment each time.

Accelerometers can vary in construction depending on the application. For high temperature applications there are accelerometers with the signal conditioning electronics built in a separate device from the actual sensor, minimizing its exposure to the temperature. There are special accelerometers for submersible applications (e.g., for below-ground structural measurements on vertical pumps) with an integrated sealed cable connection. The accelerometer can be single-axis, double-axis, and tri-axis to measure in one, two, and three orthogonal directions, respectively (i.e., x, y, and z directions simultaneously). The size of the accelerometers can also vary depending on the application and can be as small as 0.2 inches long (5.1 mm) with 0.007 oz of weight (0.2 grams). The typical accelerometer used for troubleshooting purposes is about 1 inch (25 mm) long and 0.75 inches (19 mm) Hex with about 1 oz of weight (30 grams) without the magnetic mount.

Besides vibration measurement instrumentation, there are other instruments that are useful for troubleshooting purposes, which include dynamic pressure transducers to measure pressure pulsations and piping system acoustic natural frequencies, microphones and/or hydrophones for cavitation testing, strain gauges to measure strain on casing nozzles, piping, and shafting in order to calculate stresses where failures have been experienced.

The cables used for the vibration and other type of instruments are designed to minimize electrical noise, and typically consist of twisted pairs or coaxial shielding with the shield grounded at only one end to avoid ground loops.

Vibration signal analyzers are required to provide power to the piezoelectric instruments to collect raw vibration signals initially in the time domain (amplitude versus time wave form data). Advanced analyzers further transform this complex raw signal into a typically more friendly data form of amplitude versus frequency by performing an internal mathematical operation known as the fast Fourier transform. There are several basic kinds of vibration analyzer. One type is the handheld portable analyzer, which typically has one or two channels that are commonly equipped to store the vibration data. It is used by end users to collect, on a periodic basis, routine vibration measurements to monitor the dynamic behavior of the equipment over time. The vibration data collected are part of the overall predictive maintenance program. This maintenance program usually is focused on vibration data taken at bearing housings where the interaction between the shaft natural response and the casing structure is dominant. Another type of analyzer is the multichannel analyzer, which is used for troubleshooting purposes, and typically incorporates between four to 40 channels or more in order to gather large amounts of vibration data simultaneously. Situations that would require such a large amount of data particularly occur in cases involving transient conditions during start ups, shut downs, variable speed, or load operation, etc.

The vibration analyzers are set up prior to the measurement, according to the pump condition and event to be evaluated. For instance, it requires definition of the frequency span to be recorded (typically from 1.5 Hz to 25.6 kHz), and the frequency resolution (number of lines in the frequency span, typically between 50 lines and 6400 lines), and the type of averaging (could be instantaneous or linear for a periodic and stationary condition, instantaneous or exponential averaging for a transient condition, and in some analyzers the peak-hold, which maintains the highest vibration

peaks that occur during transient conditions). In addition, the analyzer requires the input of the high pass filter setting, which is the minimum frequency of interest (e.g., frequency response that is in interest might require the DC voltage or frequency above 0.7 Hz, 7.0 Hz, or 22.4 Hz). Too low a high-pass filter setting can result in measurements that tend to “hang-up” due to constant overloading of the amplifier, combined with a long time constant for the overloaded amplifier to “clear.”

#### *Vibration Data Management—Display/Plots*

The raw waveform signal is displayed as a sinusoidal plot of vibration amplitude versus time. It is usually a very complex combination of superimposed sine waves and is used to interpret vibration behavior over relatively long periods of time or during transient events of the unit, when variations of the speed and load are present (Figure 1), or perhaps rubbing or cavitation events are occurring. The time trace allows the analyst to identify particular events related to nearly instantaneous changes in the process (system), spike events such as cavitation phenomena, etc. When the vibration event occurs periodically over time (e.g., as a function of the rotational speed), then FFT plots are more useful (experimental modal analysis being an exception, as will be discussed later). These frequency spectra are calculated in the analyzer under steady-state operation of the unit. It linearly averages a large amount of vibration samples, with each sample covering a relatively short period of time, on the order of a second or so, depending upon frequency range and the number of lines in the spectrum. The spectra allow the analyst to identify the predominant vibration peaks (discrete vibration) in terms of amplitude and the frequencies at which they occur. Simultaneously, the overall vibration can be calculated, which is basically the square root of the sum of the square (SRSS) of each individual discrete vibration amplitude within the frequency span previously selected. During predictive maintenance and most diagnostic procedures, the amplitude of these discrete peaks as well as the overall vibration are compared with specification limits that have been developed by the OEMs and/or end users for guideline purpose. These limits establish the level when the pump or the driver has reached the condition that can cause damage to their internal components. The objective of vibration specifications is to protect the equipment, and to provide a standard against which the end user, the OEM, and consulting companies can define reasonable acceptance criteria. Acceptance limits that are too loose could result in damaged machinery, while limits that are too tight are unnecessarily costly to implement since they suggest the need to modify or replace components when this is not necessary.

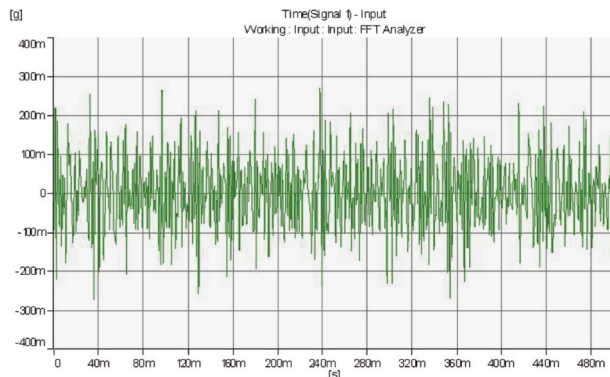


Figure 1. Vibration Waveform Signal (g's Versus Time).

The vibration amplitude output directly available from accelerometers is in g's peak or rms. End users in the Americas are more familiar with velocity units in in/s peak. The relationship between rms, peak, and peak-to-peak amplitude is shown in Figure 2.

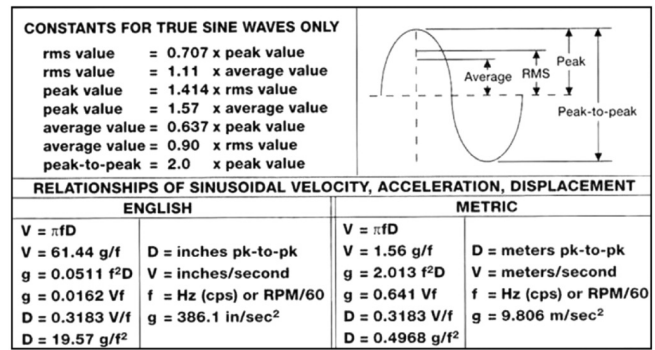


Figure 2. Vibration Sine Wave Relationships.

The scale of the amplitude can be presented in linear scale and in logarithmic scale. The linear amplitude scale is used by most vibration analysts, where the discrete vibration peaks are shown isolated with typically flat floor-noise across the frequency span (Figure 3). Often, a logarithmic scale would “inflate” the broadband floor-noise indicating key information that could be very important when performing troubleshooting, such as for example the structural natural frequencies. Figure 4 shows the same FFT plot as Figure 3, but in logarithmic scale, and through this is able to indicate the structural natural frequencies, as shown. This additional information can be curve-fit by the analyst to determine the amplification factor of the natural frequency, and to calculate the separation margin from excitation sources of the pump such as 1× fundamental harmonic of running speed, 2× rpm, vane pass frequency, etc.

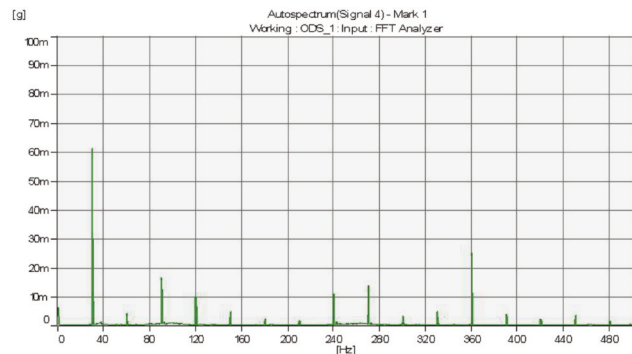


Figure 3. Vibration Spectrum in Linear Scale.

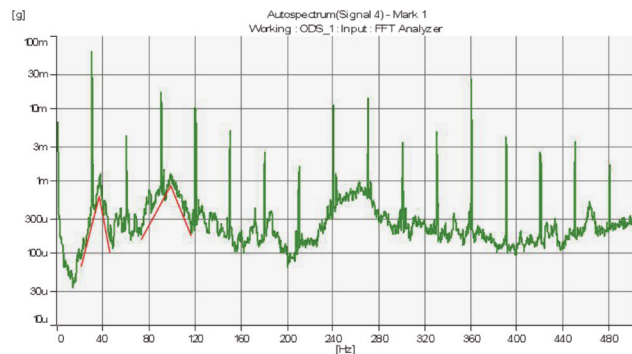


Figure 4. Vibration Spectrum in Logarithmic Scale.

Besides the FFT spectra, there are other plots sometimes used for troubleshooting purposes such as waterfall plots, which are three-dimensional (3D) plots displaying a “family” of FFT spectra along a third axis of time or in some cases versus the speed change (Figure 5). The trend plot is basically the vibration amplitude at any given frequency, or can be the overall vibration, in either case plotted along the time axis. Another type of useful plot, the orbit



plot, is created based on vibration readings from a pair of proximity probes installed on the bearing housing, monitoring the shaft and positioned in two orthogonal directions such that the polar cross-plot in time can describe the motion of the shaft center (Figure 6).

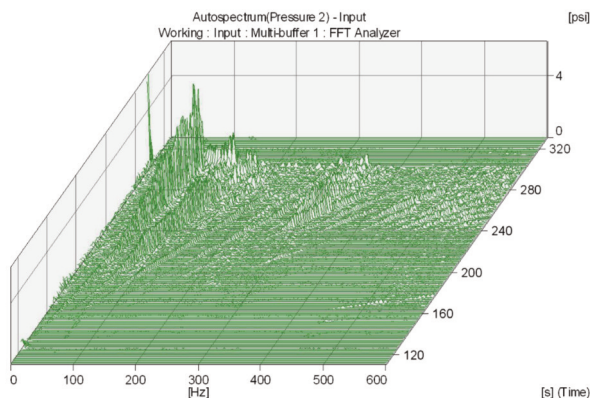


Figure 5. Waterfall Plot.

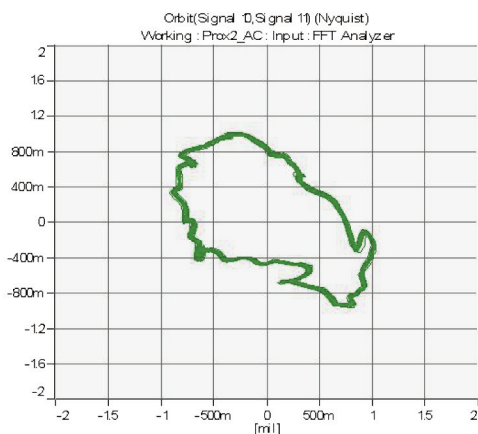


Figure 6. Orbit Plot.

## VIBRATION TESTING PRACTICE

Determining a suitable solution to chronic vibration problems has most often been performed by end users through trial and error methods, such as attempting structural fixes or progressively tightening balance tolerances on the rotors. This can be time consuming, cumulatively costly, and does not always achieve the long-term trouble-free operation that is sought. In order to achieve a high level of success in resolving vibration issues, a detailed analysis of the mechanism of the vibration problem is needed. This can be obtained by developing a finite element analysis model of the pump system, best calibrated with operating deflection shape and experimental modal analysis field vibration data, as will be shown. This combined analysis and testing approach can provide a robust platform to identify and verify the suitability of potential modifications. The identification of the root cause by this method provides a high degree of confidence that any prescribed modifications will alleviate the primary problem without creating new problems. The following section will describe the ODS and EMA vibration testing.

### Operating Deflection Shape Vibration Testing

The ODS is a thorough “natural excitation signature” vibration test performed on the entire unit structure that usually includes data collection on both the driver and the driven machinery, the associated nozzles/piping, the mounting baseplate, the foundation, and the surrounding floor (concrete) while the unit is operating under its worse-case dynamic condition (within typical operating range

condition), in order to capture the overall motion at any given frequency. In this process, it is important to gather vibration data between attachments of assembly components to capture any separation between parts (looseness, soft-foot, etc.).

To perform an ODS test, several roving accelerometers (typically tri-axis accelerometers) are used to measure the vibration signal in three orthogonal directions at a large number of representative key locations (as many as 300 to 400 measurement point/direction combinations are eventually observed, depending on the nature of the problem) along all accessible relevant structural portions of the pump and system, and often parts of any exposed or permanently instrumented shafting. Limited measurement due to access or safety reasons can be supplemented later by a test-calibrated FEA model. Figure 7 shows a typical vertical turbine pump along with data-points taken for the ODS testing. For collecting shaft vibration data, it is common to use proximity probes or temporary shaft-rider sticks equipped with mounted accelerometers to observe the shaft orbital motions (axial and torsional motions can also be detected, by special techniques). All these vibration data are recorded as amplitude versus frequency (FFT spectra), and the same data are digitally recorded versus time for a reasonable time interval (approximately one minute per measurement). The frequency span is selected depending on the nature of the problem, and it is recommended to record at least some key data at higher frequency so that it can be played-back if necessary for further investigation at various frequency ranges. The complete vibration data are taken such that one of the single accelerometer channels of the FFT signal analyzer is always kept at the same location and direction on the unit as a phase reference for each roving accelerometer, proximity probe, or other transducer (e.g., dynamic pressure transducer, microphone, or motor current transducers). The single axis reference accelerometer is usually placed where a relatively high vibration is present in the pump system across the frequency range of interest, in order to obtain a strong signal for phase angle reference.

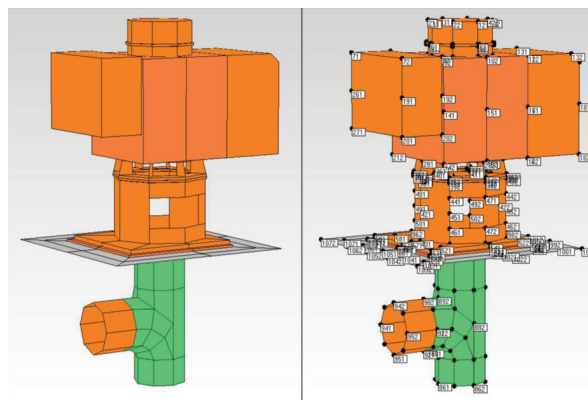


Figure 7. Pump 3D CAD Model and Vibration Data-Points from ODS Testing.

Due to the large number of vibration data-points required, it is extremely important to accurately document each measurement, identifying the location and orientation of each roving accelerometer (single and triax accelerometers), and also create a detailed drawing with the actual dimensions of the pump system to be compared with the OEM and construction drawings (if available). The field-taken dimensional sketch drawing will be used to create the 3D computer aided drafting (CAD) model for animation and troubleshooting purposes.

Each measurement is exported to the ODS database computer program. The database is arranged according to point number (later connected to a location/direction) versus frequency, amplitude, and phase angle with respect to the reference accelerometer for each data-point. In this program, each vibration data-point collected



onsite is stored in a database called the data block, then this data block is assigned to the 3D model (e.g., CAD model) of the pump system tested, maintaining the same data-point location and orientation (horizontal-vertical-axial). The global CAD model is constructed by laying out various substructures within the system such as the motor, pump bearing housings, pump casing, baseplate (and for vertical turbine pumps, discharge head and column pipe), foundation, floor, etc. Each substructure is created from single points, lines, and surfaces. Once the field information is assigned, each substructure or group of substructures is selected to apply interpolation equations to assign relative motion to those points that do not have actual vibration data. In this way, each component or substructure in the model will have an independent self-defined motion when measurement between independent parts has been gathered to observe potential looseness or separation between parts.

Once the measurement assignment and interpolation equations are applied to each substructure, the model can be evaluated at any given frequency. From the field testing, the highest discrete vibration amplitude has already been detected at key frequencies, which are usually the excitation sources such as  $1\times$  rpm (typically for imbalance),  $2\times$  rpm (typically for misalignment), impeller vane pass frequency (VPF), diffuser vane pass frequency, gear mesh frequency (GMF, when gears are present), subsynchronous peaks (e.g., for shaft rubbing, or rotating stall), etc. It is typically best to evaluate first the ODS model at the running speed of the pump. The resulting vibration animation describes in exaggerated motion/deformation (but consistently scaled) the pump vibrational motion at the selected frequency in order to easily identify for example the “weakest” location of the pump, which in the example in Figure 8 experiences vibration levels above specifications.

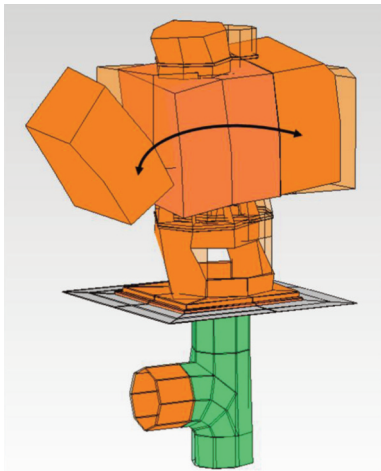


*Figure 8. Pump ODS at the Running Speed Rocking in the Parallel Direction to the Discharge Pipe.*

If the excitation frequency source is close to a natural frequency, the ODS animation at this natural frequency would describe an approximate mode shape of the natural frequency. Modes that historically have been clearly evident from their shapes include first, second, and third bending modes of long cantilever structures, horizontal and axial rocking rigid body modes, vertical bouncing modes, torsional modes, etc.

In order to increase the separation margin between the excitation source and the structural natural frequency, there are typically two alternatives, depending on the case, to shift the natural frequency. One is increasing or decreasing the stiffness of the system to shift upward or downward the natural frequency. The other one is adding mass to shift downward the offending natural frequency. In order to avoid “trial and error” process to detune a natural frequency in this manner, the FEA analysis approach, described later, is considered a very good additional tool.

### *Experimental Modal Analysis*

Similar in some respects to ODS testing at nonsynchronous frequencies, EMA is a type of “impulse-response” test to determine the structural natural frequencies and the mode shapes of the pump system by using an instrumented hammer instead of the natural excitation of the pump. Therefore, the response of the machinery is measured through the accelerometers from a known input excitation source (e.g., instrumented hammer for a broadband-excitation impact). An engineered impact hammer is provided with different materials to be placed at its tip (i.e., various hardness of rubber material, or even metals such as bronze) depending on the frequency response that is required (harder tips excite higher frequencies). It is known that the response of the hammer will decay (roll-off) for response at higher frequency; therefore the tip should be selected such that the natural frequency of interest would fall within frequency span before first roll-off. For each measurement/accelerometer location, a number of impacts should be applied until the average of frequency response spectra becomes steady. Typically, if the machine is not operating, the impact number per test is about 10 to 15.

Since the natural frequencies are usually inline with the principal axes of the pump, this EMA test is performed in three orthogonal directions (horizontal, vertical, and axial direction) by impacting the pump component near where the highest vibration was detected during natural excitation test. Modal testing is typically performed by plants and OEMs when the pump is not operating. However, whenever practical it is recommended to perform this test by using a method such as a modal analysis technique that can effectively determine critical speeds and structural natural frequencies of all rotating machinery under operating conditions, such that “bump testing” is performed without shutting down the equipment. This technique is especially useful in multistage high energy variable speed pumps whose rotordynamic characteristics are strongly speed and load dependent. This test takes into account the added mass effect of pumped fluid entrapped in the pump casing, the energized bearing and Lomakin Effect seal stiffnesses, and the gyroscopic effect due to the rotational speed of the rotor. Therefore, it properly accounts for the boundary conditions established by the operating condition. Also, it is able to identify any natural frequency related problems without any downtime of the tested pump or nearby equipment, which can be important in many applications and industries.

This technique incorporates time averaging statistics to rapidly improve the signal-to-noise ratio under operating conditions. Time averaging reduces the amplitude ratio of the random naturally excited vibration versus the impact-coherent vibration during the signal processing to greatly emphasize the effect of the “bump” while the machine continues its normal operation. Since the natural excitation from the pump is present, this technique requires a large amount of impacts in order to average-out and cancel the main and often strong excitation sources such as  $1\times$  rpm,  $2\times$  rpm,  $1\times$  VPF,  $2\times$  VPF, etc.

### FINITE ELEMENT ANALYSIS

Once the ODS and the EMA animations are created and analyzed at particular frequencies, an FEA model is constructed and calibrated to match the problematic frequencies and mode shapes uncovered in the vibration test data. The FEA model incorporates the actual dimensions of the pump parts and is typically constructed and assembled from two-dimensional (2D) drawings or physical measurements using a computer-generated (CG) solid-modeler. Each part in the model is assigned appropriate material properties taking into account any water mass effects, including external added mass effects due to submerged columns such as found in vertical turbine pumps. The model includes the appropriate foundation and nozzle constraints, shafting geometry, impeller inertia properties, and a motor representation based on its weight, CG, and manufacturer-supplied reed frequency. Once the

model has been calibrated to the data, proposed virtual fixes such as adding ribs or weight or removing material can be simulated using the FEA model to determine the best course of action to rectify or mitigate the vibration problem. Typically, as a minimum, an increase in separation margin of at least (10 percent to 15 percent) is desired and can normally be achieved with a high degree of confidence using field test data and a well calibrated finite element model.

#### FEA Fundamentals

The detailed numerical concepts concerning the finite element technique are beyond the scope of this tutorial, and the reader is advised to refer to the literature, which contains numerous books, articles, and papers on the subject. Nevertheless, some mention of the basic finite element concepts will be discussed to give the reader some background to the method. Essentially, the finite element method attempts to simulate the behavior of a structure by representing it with many smaller well understood components or elements. The stiffness matrix of a small rectangular element with four corner nodes in the case of a 2D shell element or eight corner nodes in a 3D brick element is well understood mathematically. The process of breaking down a structure into typically thousands of these well-understood elements is called the meshing process and is often done automatically by present day finite element codes. The assembly of these elements at the node points allows for an overall stiffness matrix, and in the case of a modal analysis a mass matrix as well to be created that represents the entire structure. The finer the breakup of the structure, the more precise the results will be. In addition to 3D solid elements, shell elements that have a thickness input are often used to model large diameter, thin walled structures such as pump columns and discharge heads. Beam elements, where cross sectional properties are input, can be used for shafts, piping, or struts, and mass and spring elements, which are often used to model impellers and bearing stiffnesses, respectively. They are also widely used in finite element models to simulate portions of the actual pump. The solution to these large assembled matrices of finite elements, which involves numerical method calculations of inverted matrices, is performed transparently to the user. In case of the modal analysis, the output will be a list of natural frequencies along with the corresponding mode shapes of each determined frequency.

#### CASE HISTORY 1

A barrel type pump in charge service at a nuclear power plant facility had been exhibiting elevated vibrations that were highly erratic in amplitude and phase angle (relative to shaft position) during normal monitoring. It was speculated by plant personnel that this behavior could have been attributed to a possible crack, which might have developed in the shaft due to an event experienced in the previous year. During that event, normal electrical power was lost, and the motor was suddenly restarted when the plant's diesel generator came online. To prevent a potential failure or intervention by the Nuclear Regulatory Commission (NRC) leading to costly downtime, the personnel had planned a complete teardown of the pump in order to perform a visual inspection of the shaft. However, it was later decided that the pump should undergo extensive field vibration testing rather than a costly internal inspection to determine if a cracked shaft was responsible for the erratic vibration behavior.

#### Field Vibration Testing

The maximum vibration amplitude of approximately 0.22 in/s (5.59 mm/s) peak was detected in the horizontal direction on the outboard bearing housing at  $1\times$  pump operating speed of 4812 rpm (80.2 Hz), as shown in Figure 9. However, the sister pump had a similar deflection shape at the running speed, but the maximum horizontal vibration level on the outboard bearing housing measured was only 0.054 in/s (1.37 mm/s) peak.

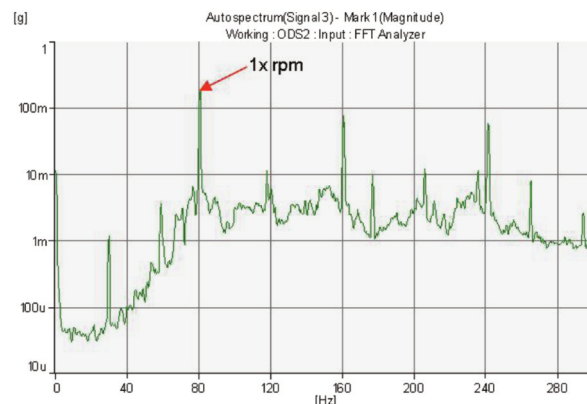


Figure 9. FFT Plot of the Outboard Bearing in the Horizontal Direction (0.2 g's or 0.22 in/s peak at 80.2 Hz).

The operating deflection shape showed that the pump was rocking from side to side, and most importantly, that one of the outboard pump feet had a loose connection to the pedestal ("soft foot") as shown in Figure 10. Experimental modal analysis performed on the pump while stationary indicated a strong natural frequency at 93 Hz (Figure 11) in the horizontal direction, which was considered adequate (16 percent of separation margin above the running speed). However, when the EMA test was performed using an experimental modal analysis technique during pump operation, the actual natural frequency was detected at 76.2 Hz, which had only 5 percent separation margin from the running speed amplifying the vibration in the horizontal direction (Figure 12).

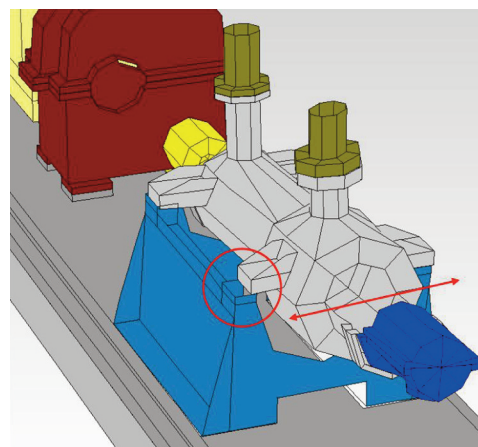


Figure 10. Barrel Pump ODS at the Running Speed.

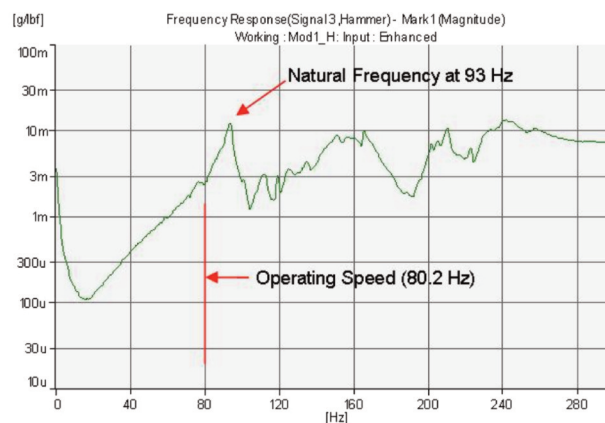


Figure 11. Frequency Response Spectrum from EMA Testing While the Pump Was Not Operating.

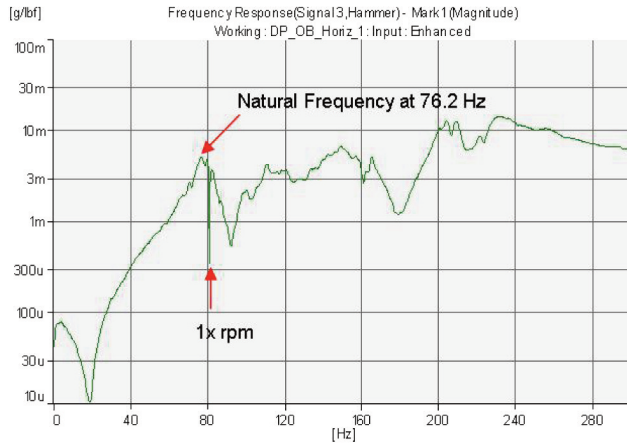


Figure 12. Frequency Response Spectrum from EMA Testing While the Pump Was Operating.

#### FEA Analysis and Results

At the plant management's request, before any corrective action by the plant, the authors performed a finite element analysis (Figure 13) to simulate the structural behavior of the pump on its pedestal for conditions with and without the soft foot. The analysis with all four feet securely connected to the pedestals predicted a natural frequency similar to that observed in the stationary modal test. The analysis was fine-tuned to accurately match the 93 Hz structural natural frequency and mode shape of the pump as determined through impact modal testing (Figure 14). The same model was analyzed with the "soft foot" condition, which showed that the same natural frequency shifted lower to 78 Hz (Figure 15) close to the running speed of 80.2 Hz. This calculated natural frequency was also very close to the natural frequency detected experimentally (approximately 2 percent difference). Therefore, the FEA model was considered calibrated with the field test data.

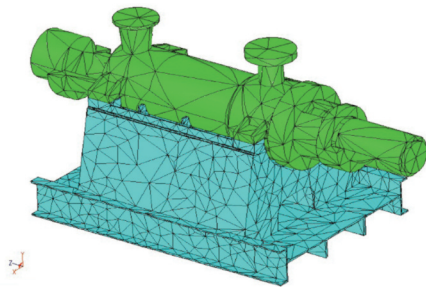


Figure 13. FEA Model for the Barrel Pump, Using Large but Accurate "Polynomial" Elements.

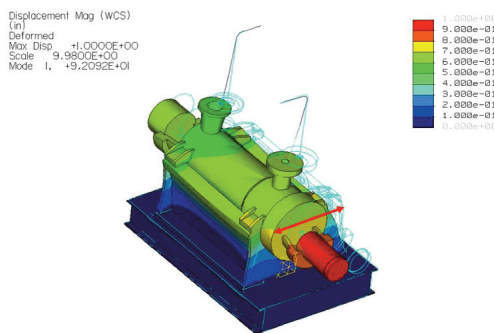


Figure 14. FEA Calculated Mode Shape of the Pump (92.1 Hz) with All Bolted Foot Connections Secure.

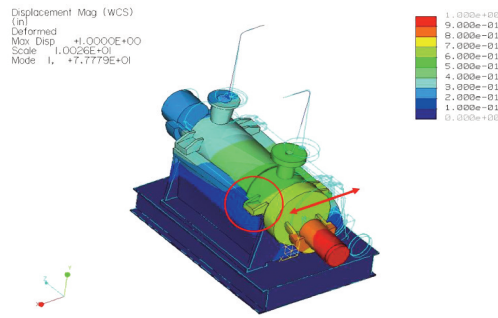


Figure 15. FEA Calculated Mode Shape of the Pump (77.8 Hz) with the Simulated "Soft Foot" on One Outboard Foot.

This structural natural frequency at approximately 76.2 Hz was changing somewhat from start to start and also during steady operation depending upon the stiffness of the bolted connection. This shift resulted in the pump tuning in slightly better or worse with the natural frequency, which affected the amplification and the phase angle of the vibration. Correcting the "soft foot" condition eliminated the variations in amplitude and phase measured on the outboard bearing housing. In addition, there was no evidence of shaft cracking in further vibration analysis. The considerable cost of an extensive maintenance repair operation was avoided.

#### Conclusions and Recommendations

- The ODS of the pump at 80.2 Hz showed a rocking motion of the pump and clearly indicated that there was motion of one of the outboard pump feet (on the left side when viewed from the nondrive-end of the pump) relative to the pedestal on which it was mounted. This relative motion was indicative of a loose connection or "soft foot" on the pump.
- The stiffness of the pump support connection was varying from start to start as well as during steady operation, thereby causing the natural frequency to shift. Therefore, the variations in vibration amplitude and phase were a result of this natural frequency tuning in and out of the pump running speed. This shift in natural frequency and its effects was confirmed with finite element analyses of the pump with and without the soft foot.
- In situations such as this, the bolted connections of the pump casing to the baseplate pedestals should be inspected for soft foot condition and corrected as necessary. The torque value for the bolt on the soft foot should be recorded in its "as-found" condition as well as after being properly tightened to the manufacturer's specifications. Prior to loosening the hold down bolt, dial indicators should be placed on the foot, and the displacement of the foot recorded as the bolt is loosened. If necessary, shims could be used to take up any gaps between the pump foot and the pedestal.

#### CASE HISTORY 2

Two circulation vertical turbine pumps with 45 ft (13.72 m) long column assembly installed in a nuclear facility were presenting premature wearing of the line shaft bearings and shaft sleeves leading to frequent and costly repairs. Vibration amplitude was reported to be variable depending on the level of the lake where the pumps were installed.

#### Field Vibration Testing

During the vibration testing performed, the maximum vibration above-ground was measured to be approximately 0.39 in/s (9.91 mm/s) peak at the running speed of 14.9 Hz (894 rpm) in the direction perpendicular to the discharge pipe (Figure 16). A below-ground accelerometer located above the suction bell flange, in the same direction, was indicating 0.74 in/s (18.8 mm/s) peak at the same frequency (Figure 17).



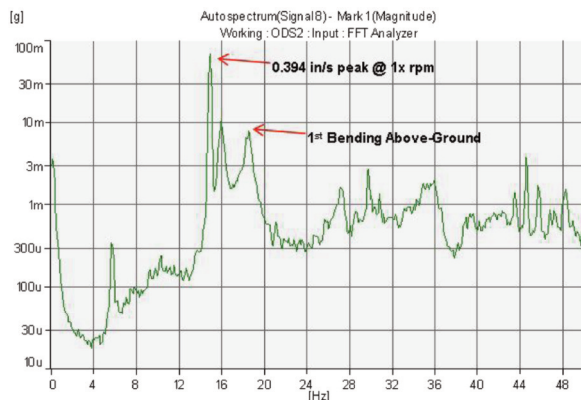


Figure 16. Vibration Spectrum (FFT) Measured at the Top the Motor in the Perpendicular Direction to the Discharge Piping.

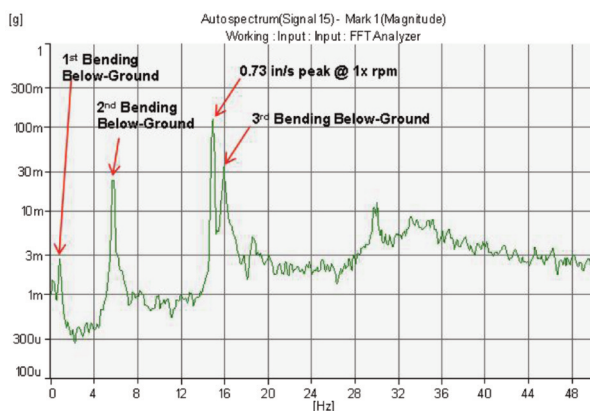


Figure 17. Vibration Spectrum (FFT) Measured at the Column Below-Ground in the Perpendicular Direction to the Discharge Piping.

From these vibration spectra, with the amplitude plotted with logarithmic scale the natural frequencies were able to be identified by their wide peaks within the broadband noise-floor. Therefore, based on above- and below-ground measurements, the main natural frequencies were able to be identified as shown in Table 1. From the below-ground measurement the same natural frequencies were detected as were obtained on the motor (much more weakly on the motor for the first mode) with the addition of a natural frequency at 0.75 Hz. Therefore, the closest natural frequency to the running speed had less than 7.0 percent separation margin (15.9 Hz versus 14.9 Hz), while typical separation margin required is between 10 percent to 15 percent, especially with respect to a  $1\times$  running speed excitation source. The natural frequencies in the parallel direction to the discharge piping were the same or higher as expected, due to the stiffness provided by the piping in this direction.

Table 1. Structural Natural Frequencies and Mode Shapes from ODS Testing.

Mode Shape	Natural frequency parallel to the discharge pipe (Hz)	Natural frequency perpendicular to the discharge pipe (Hz)
1 <sup>st</sup> bending below-ground	0.75	0.75
2 <sup>nd</sup> bending below-ground	5.75	5.75
3 <sup>rd</sup> bending below-ground	15.9	16.0
1 <sup>st</sup> bending above-ground	18.6	18.5

Experimental modal analysis performed while the pump was not operating indicated that the natural frequencies shifted upward because the added water mass effect inside the column pipe and discharge head was not present. Table 2 summarizes the natural frequencies and their mode shapes.

Table 2. Structural Natural Frequencies and Mode Shapes from Nonoperating EMA Testing.

Mode Shape	Natural frequency parallel to the discharge pipe (Hz)	Natural frequency perpendicular to the discharge pipe (Hz)
1 <sup>st</sup> bending below-ground	0.88	0.88
2 <sup>nd</sup> bending below-ground	6.40	6.50
1 <sup>st</sup> bending above-ground	18.1	17.4
3 <sup>rd</sup> bending below-ground	21.9	21.6

Since the below-ground structure was only instrumented with one pair of submersible accelerometers at the suction bell flange (in orthogonal direction), it would be difficult to identify the mode shapes based on test alone. However, a combination of the ODS animations, authors' experience, and FEA analysis results enabled the mode shapes to be accurately characterized. The animations created from the ODS testing clearly revealed that the first bending below-ground (primarily) natural frequency was at 0.75 Hz (Figure 18), and the above-ground mode (primarily motor cantilever) was identified at approximately 18.6 Hz (Figure 19). In theory, for cantilever beams, the second and the third bending natural frequencies are expected to be approximately 6.3 and 17.5 times, respectively, of the first bending frequency (for uniform area moment of inertia along the beam structure). Therefore, the second and third modes were expected to be correspondent with measured natural frequencies at 5.75 Hz and 16.0 Hz, respectively, approximately similar to the test results. These natural frequencies were confirmed later with the FEA analysis.

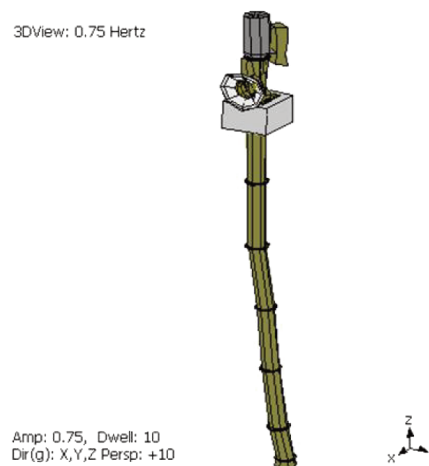


Figure 18. ODS at 0.75 Hz Showing the First Bending Below-Ground.

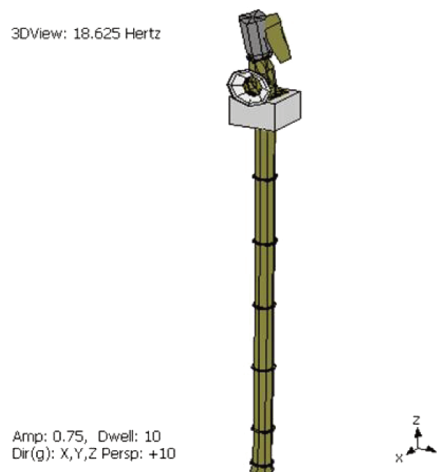


Figure 19. ODS at 18.6 Hz Showing the First Bending Above-Ground.

### FEA Analysis and Results

A detailed FEA model created of the pump assembly was calibrated with the field test results of natural frequencies above- and below-ground. This calibration was carried out by, first, tuning the motor with its reed frequency (fixed at the mounting flange) along with the actual mass and the CG provided by the motor manufacturer. The second step involved changing the pump components' density by taking into account the added water mass inside the column pipe and discharge head as well as the water level outside the pump. The third step involved including part of the concrete foundation to take into account its flexibility as well as the stiffness of the mounting support or the soleplate. Figure 20 shows the solids and FEA model of the pump assembly.

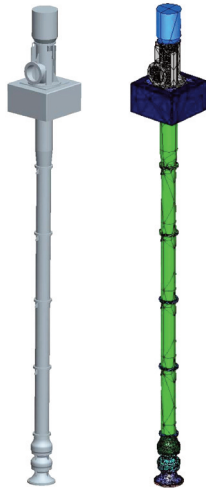


Figure 20. Solids and FEA Model for the Two-Stage VTP.

From the FEA results, by calibrating the first bending modes (above- and below-ground), the second and third bending below-ground were predicted to be at 5.9 Hz and 16.7 Hz, which were close to the measured natural frequencies at 5.75 Hz and 16.0 Hz (3 percent to 4 percent difference). Figures 21 through 24 show the FEA results for each natural frequency registered in the field testing. The FEA model was also used to verify that natural frequency of the third bending mode shifted downward (closer to the running speed) when the water level increases.

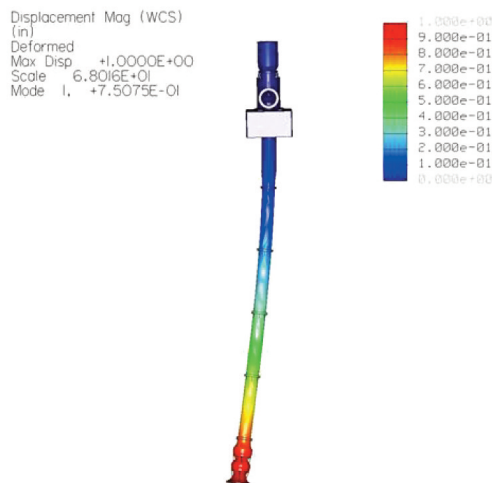


Figure 21. FEA Predicted First Below-Ground Bending Mode Shape at 0.75 Hz.

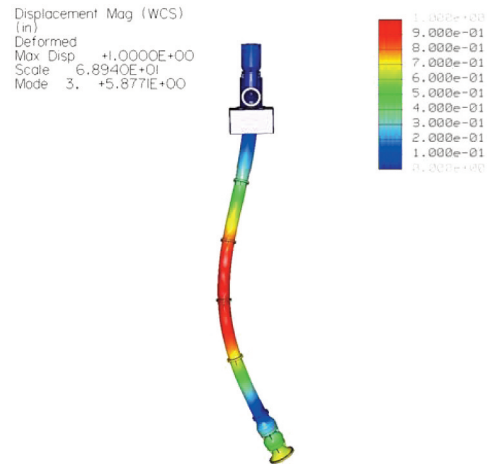


Figure 22. FEA Predicted Second Below-Ground Bending Mode Shape at 5.9 Hz.

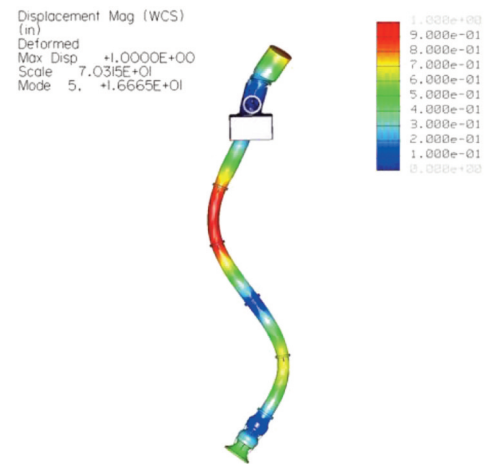


Figure 23. FEA Predicted Third Below-Ground Bending Mode Shape at 16.7 Hz.

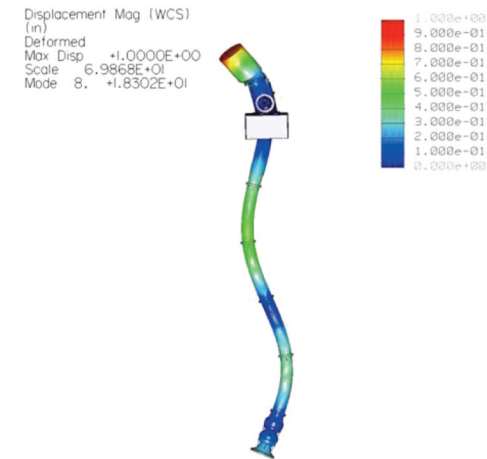


Figure 24. FEA Predicted First Above-Ground Bending Mode Shape at 18.3 Hz.

Once the authors confirmed the mode shape of each natural frequency, the ODS model was able to be modified by including additional vibration data for the below-ground structure at several elevations of the column pipe with amplitudes and phase angles based on the actual measurement in order to reproduce the third

bending mode and the ODS motion at the running speed. The shape of the  $1\times$  ODS was expected to be similar to the natural frequency as shown in Figures 25 and 26, respectively, due to their proximity to each other.

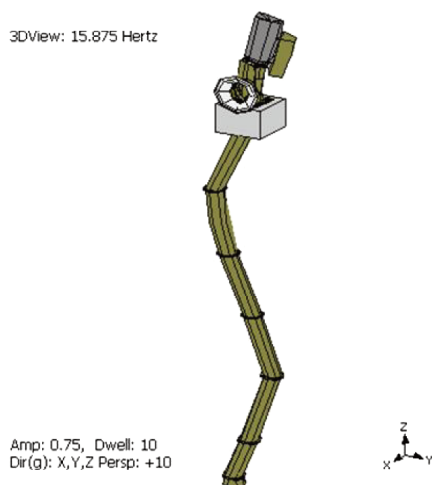


Figure 25. ODS at 15.9 Hz Showing the Third Bending Below-Ground.

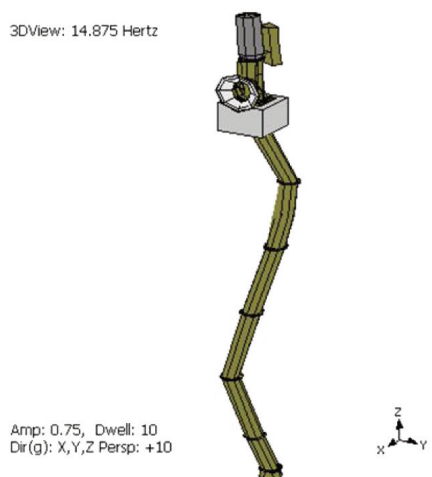


Figure 26. ODS at the Running Speed of the Pump (14.9 Hz).

#### Conclusions and Recommendations

- The third bending mode structural natural frequency of the column pipe was detected at approximately 7 percent above the running speed of the pumps and was the cause of the increased vibration at  $1\times$  running speed. This natural frequency was expected to get even closer to the running speed following any increment in the level in the lake adding more external mass on the wet column pipe section.
- Recommendations to improve the vibration levels of the above- and below-ground structure included welding 1.0 inch thick ribs along the upper portion of the column pipe. This would shift the third bending mode approximately 16 percent. Figure 27 shows the expected natural frequency (19.3 Hz) and the mode shape.
- The second option consisted of removing a section of column pipe (this was hydraulically acceptable). This modification would shift upward the third bending mode structural natural frequency of the column pipe approximately 48 percent. Figure 28 shows the expected new natural frequency (24.7 Hz) and the mode shape.

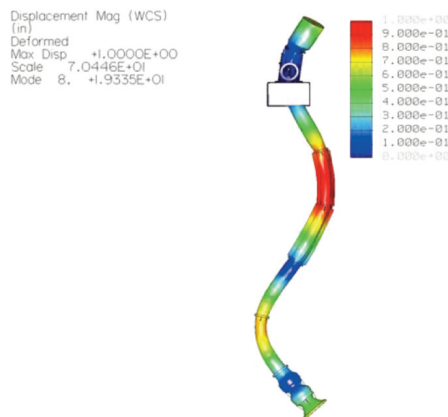


Figure 27. FEA Predicted Third Below-Ground Bending Mode Shape at 19.3 Hz by Adding Ribs at the Midsection of the Column Pipe Assembly.

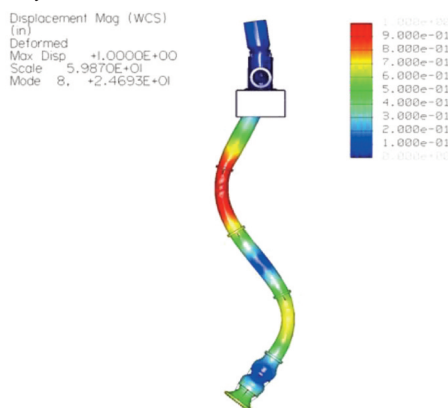


Figure 28. FEA Predicted Third Below-Ground Bending Mode Shape at 24.7 Hz by Removing a Section of the Column Pipe Assembly.

#### CASE HISTORY 3

Two vertical turbine can-style condensate pumps were undergoing routine maintenance in a fossil power plant. Upon returning one of the pumps to service, high vibrations were being measured at the top of the motor, while the sister pump, which had not undergone maintenance, was not experiencing the high vibrations. The pumps had been in service for over 40 years, but the monitoring of the motor vibrations had only recently begun as part of the plant's overall maintenance program. The motors were supported by a stand that consisted of six vertical angle iron beams that allowed access to the coupling from many points around the support. Figure 29 shows a picture of the pump.



Figure 29. Vertical Turbine Canned Pump Motor Supported on the Stand.



### Field Vibration Testing

Accelerometer data taken at the top of the motor of the refurbished pump indicated a strong response at  $1\times$  running speed as shown in the spectrum in Figure 30. The vibration was nearly 1.1 in/s (27.9 mm/s) peak, and a natural frequency at running speed was the likely source of the high vibration due to the width of the peak. The modal tests confirmed that the first above-ground structural natural frequency was indeed equal to  $1\times$  running speed of 1185 rpm (19.75 Hz), and the EMA frequency response spectrum is shown in Figure 31, indicating a strong resonant condition. ODS plot at the running speed is shown in Figure 32. The shape of this ODS demonstrated that the motor stand was considerably more flexible than the pump can.

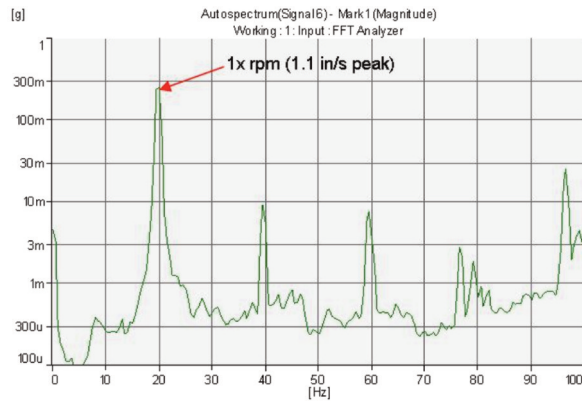


Figure 30. Vibration Spectrum (FFT) Measured at the Top of the Motor in the Perpendicular Direction to the Discharge Piping.

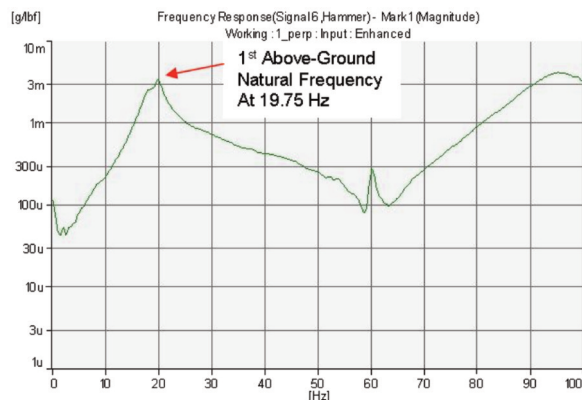


Figure 31. Frequency Response Spectrum from EMA Testing While the Pump Was Not Operating Measured at the Top of the Motor in the Perpendicular Direction to the Discharge Piping.

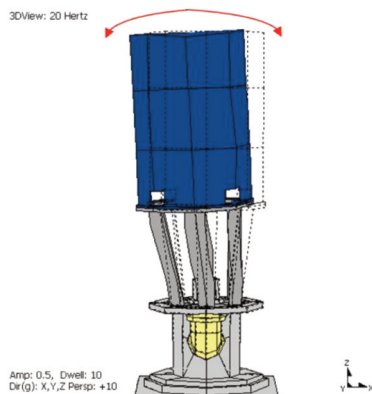


Figure 32. ODS at  $1\times$  RPM of the Pump Showing the First Bending Above-Ground.

In order to reduce the vibrations to an acceptable level, the stiffness or the mass of the pump assembly had to be adjusted to shift the natural frequency and avoid a resonance condition. Onsite testing showed this approach was successful by adding sufficient weight to the top of the motor (670 lb/304 kg), which reduced the natural frequency to 17.00 Hz (Figure 33) and lowered the vibration levels perpendicular to the discharge piping from 1.1 in/s (27.9 mm/s) peak to 0.21 in/s (5.33 mm/s) peak. The ODS spectrum is shown in Figure 34, and it is clear that the natural frequency with the added weight has shifted below  $1\times$  rpm by the two distinct peaks, whereas previously under normal operating conditions, the  $1\times$  rpm spike was sitting directly on top of the natural frequency peak.

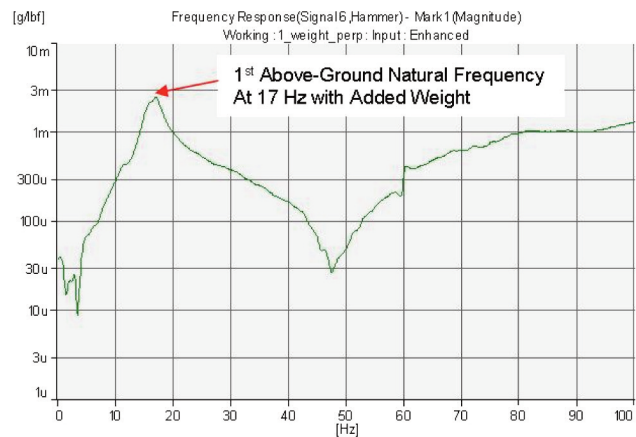


Figure 33. Frequency Response Spectrum from EMA Testing While the Pump Was Not Operating Measured at the Top of the Motor in the Perpendicular Direction to the Discharge Piping and Adding 670 Lb to the Top of the Motor.

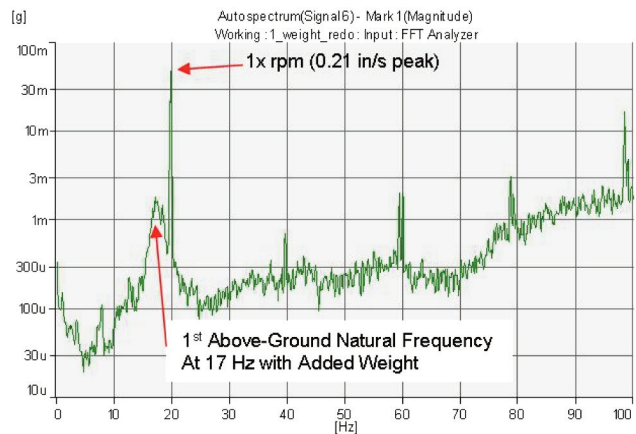


Figure 34. Vibration Spectrum (FFT) Measured at the Top of the Motor in the Perpendicular Direction to the Discharge Piping.

At first glance this appeared to be a simple vibration problem with a quick fix, however, similar data taken on the sister pump, which had not been refurbished, indicated that the first bending natural frequency above-ground was much less at 17.9 Hz. The flange bolting was tight in both pumps, and the motors and motor stands were identical. Normally, shafting is very flexible in vertical pumps and packing offers little in the way of stiffness, but still something was accounting for the 10 percent difference in natural frequency between the pumps. There was no leakage coming from the stuffing box on the problematic pump, but a fair amount of leakage was coming from the sister pump. Another onsite impact test was performed on the problematic pump,

uncoupled from the motor, and surprisingly the natural frequency dropped from 19.75 Hz to 18.4 Hz. Clearly, the shafting and packing were having an effect on the natural frequency in these pumps, which is highly unusual. This is not normally seen on more standard vertical pumps with cylindrical discharge heads with limited expanse access windows. The natural frequencies of the motor/discharge head are not affected by the shafting with this type of motor support. Although adding weight reduced the natural frequency and vibration levels, it was used only as a diagnostic tool and not a permanent solution, so a detailed FEA analysis was conducted to evaluate effective structural modifications to resolve the natural frequency issue with a high degree of confidence for success.

#### FEA Analysis and Results

The computer solid modeling was done with a commercially available solids modeler, and the modal FEA was completed using an integrated finite element code associated with the modeler. Solid models of the motor, supports, portions of the pump can, shaft, and stuffing box were created according to measurements taken onsite and from discussions with plant personnel. The modal properties of the pump assembly were matched to the test results at three conditions—full assembly, with the shaft disconnected, and with additional weight on top of the motor. This ensured the FEA model was accurately representing the pump as installed onsite, so that the analysis could confidently predict the effects of a proposed solution.

The solid model of the pump assembly needed to perform the FEA of the structure is shown in Figure 35. The first step was to match the properties of the motor model to common values for a reed frequency and center of gravity location. Then the motor was added to the discharge head supports and the section of the pump can that was above ground so the FEA natural frequency could be checked without any effects of the shaft and stuffing box. The resulting natural frequency of 18.4 Hz closely matched the test data, and the FEA mode shape is shown in Figure 36 (motor uncoupled). Next, the model was run with the shaft and stuffing box connected to correctly identify the stiffness contribution of these parts. The mode shape is shown in Figure 37, and the frequency of 19.8 Hz matched the test data. After the model was matched at these two conditions, the 670 lb (304 kg) plates were added to the top of the motor. The resulting FEA frequency was 17.2 Hz, matching the field test results, and is shown in Figure 38. These three steps proved that the FEA model was an accurate representation of the pump assembly as installed in the field. This was important so that the effects of any proposed solution could be accurately quantified.

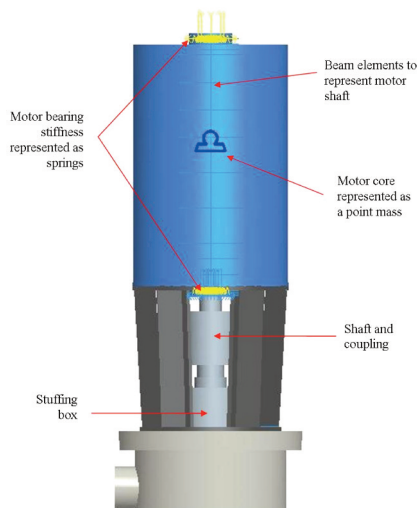


Figure 35. Solids and FEA Model for the Canned VTP.

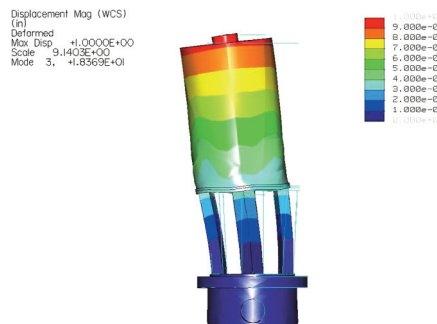


Figure 36. FEA Predicted First Above-Ground Bending Mode Shape at 18.4 Hz by Uncoupling the Motor (without Shaft Effect).

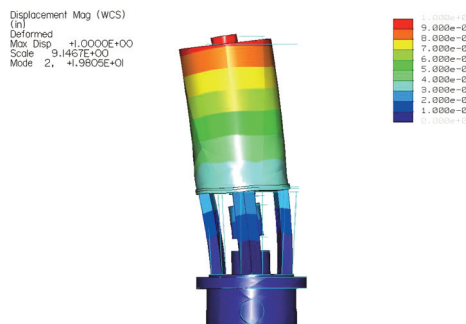


Figure 37. FEA Predicted First Above-Ground Bending Mode Shape at 19.8 Hz by Coupling the Motor (with Shaft and Stuffing Box Effect).

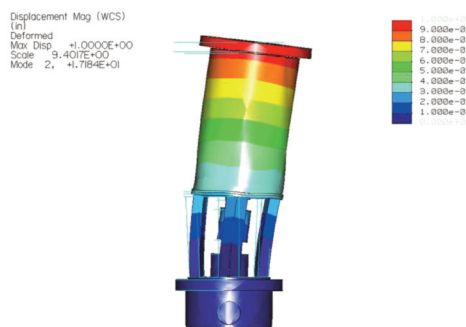


Figure 38. FEA Predicted First Above-Ground Bending Mode Shape at 17.2 Hz by Adding 670 Lb of Weight on Top of the Motor.

After discussions with the plant, a proposed solution to increase the stiffness of the discharge head supports (but one that would still allow for routine maintenance) was evaluated using the FEA model. The solution was to wrap a curved plate around the existing vertical beams with sufficient sized cutouts for access to the coupling. The additional structural supports were then modeled and added to the FEA assembly to determine the resulting natural frequency increase. The FEA model with a 1/2 inch (12.7 mm) wall thickness plate around the motor stand is shown in Figure 39. A modal analysis was completed, and the natural frequency increased to 26.6 Hz, or 35 percent separation margin from the running speed, and the resultant mode shape is shown in Figure 40. The analysis was rerun with varying values for the stiffness of the packing within the stuffing box because as this clearance grows (i.e., packing wears over time) the reduced stiffness will lower the natural frequency closer to running speed and risk resonance. The analysis indicated that the proposed solution was successful in maintaining a minimum 24.7 percent separation margin from running speed in either direction, even when the stuffing box is not providing any stiffness to the system. This alleviated any concerns that the effectiveness of the additional supports would decrease as the stuffing box packing

wears. The proposed solution was also evaluated with a wall thickness of  $\frac{3}{4}$  inch (19 mm), and the natural frequency increased only an additional 4.2 percent in the worst case scenario of the stuffing box providing no stiffness. A surprising result given the 50 percent increase in the thickness of the plate. Therefore, it was recommended that the  $\frac{1}{2}$  inch (12.7 mm) thick plate be used because of diminishing returns with increased wall thickness. This also underscores the usefulness of the FEA to guide the engineers to a practical cost-effective solution.



Figure 39. FEA Model for the Canned VTP with  $\frac{1}{2}$  Inch (12.7 MM) Thick Plate.

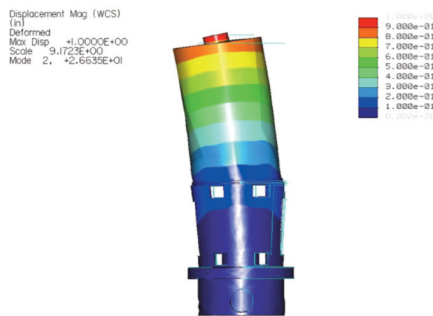


Figure 40. FEA Predicted First Above-Ground Bending Mode Shape at 26.6 Hz by Welding  $\frac{1}{2}$  Inch (12.7 MM) Plate Around the Motor Stand.

#### Conclusions and Recommendations

- There was a natural frequency of the motor and motor support structure on the above-ground structure of the pump at 19.75 Hz in the direction perpendicular to the discharge piping, which was in resonance with the  $1\times$  running speed of the unit.
- When the pump was uncoupled from the pump, impact testing indicated the natural frequency of the pump dropped to 18.25 Hz. This implied that the stuffing box was providing stiffness along with the shaft. FEA results also confirmed this behavior. Furthermore, the natural frequency of the sister pump was determined from impact testing to be 17.9 Hz, and was exhibiting much more leakage through the stuffing box packing, which was an indication that the stuffing box most likely was not providing the same stiffness as the problematic pump, which was recently refurbished.
- Incorporating the additional  $\frac{1}{2}$  inch (12.7 mm) thick plate around the motor stand would increase the structural natural frequency beyond 15 percent above  $1\times$  running speed even if the stiffness due to the packing were to diminish over time.

#### CASE HISTORY 4

Three newly installed vertically mounted sewage pumps with two-vaned impellers were driven by long drive shafts with U-joints. They were experiencing very high pump bearing tower vibrations at vane pass frequency, nearly over the entire speed range of the units. The pumps were operating between 1200 rpm (20 Hz) and 1800 rpm (30 Hz) via a variable frequency drive (VFD) controlled motor located on a separate floor above the pumps. The single cutwater volute pump casings were supported by individual fabricated steel stands that were anchored to the floor at four hold down locations. Figure 41 shows a photo of the pump arrangement.



Figure 41. Sewage Pumps Mounted on Fabricated Stands.

As with the previous case study, field testing of the pumps consisted of a combination of impact modal testing as well as operating forced response testing. Data for each of these tests were acquired at numerous locations on the motor, motor stand, pump, pump stand, foundation, and piping for all the pumps. Impact modal testing was used to determine the natural frequencies of the motors, drive shafts, and pump casing/pump stand. The operating forced response test data were used to produce the operating deflection shape of the pumps to help visualize the mode shapes of the problematic frequencies.

#### Field Vibration Testing

Accelerometer data taken at the top of the motors indicated that the motors did have natural frequencies around 30 Hz that were resulting in elevated  $1\times$  running speed vibrations at the maximum speed of 1800 rpm; however, these vibrations were easily reduced by simply stiffening the motor support stand. FEA of the motor and stand provided a quick and effective solution to the motor vibration problems so they will not be discussed. The focus of this case study will now turn to the pumps, which were experiencing much greater and more complex vibration issues. Since all three pumps were experiencing approximately the same levels of vibrations, this discussion will only concentrate on one of the pumps as the solution that was eventually conceived was applied to all three. Accelerometer data taken on the pump bearing tower in the parallel and perpendicular direction are displayed in Figures 42 and 43 while the pump was operating at the maximum speed. The vibration amplitude at the running speed ( $1\times$  rpm) was well within specification; however, the second harmonic or vane pass frequency discrete vibration was excessive (1.75 in/s [44.5 mm/s] peak and 1.16 in/s [29.5 mm/s] peak) in the parallel and perpendicular directions to the discharge piping, respectively. From the FFT spectra plots some natural frequencies were easily identified at 39.5 Hz, 47.3 Hz, and 50.4 Hz. However, there was no clear evidence of a resonance condition at  $2\times$  running speed frequency.



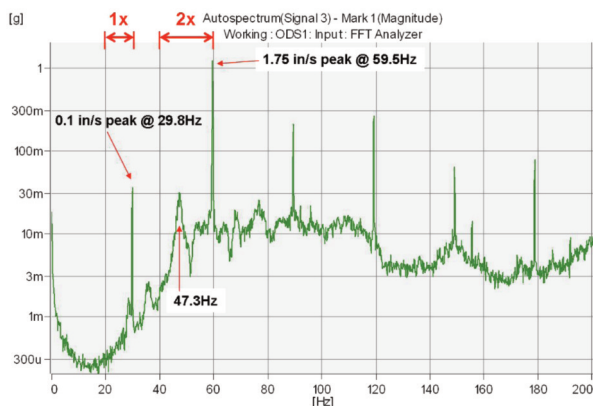


Figure 42. Vibration Spectrum (FFT) Measured at the Top of the Bearing Tower in the Parallel Direction to the Discharge Piping.

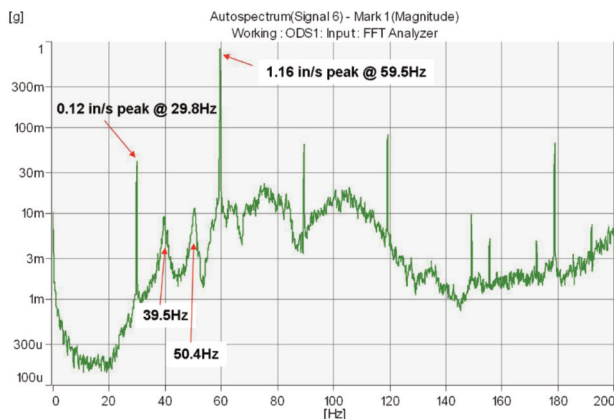


Figure 43. Vibration Spectrum (FFT) Measured at the Top of the Bearing Tower in the Perpendicular Direction to the Discharge Piping.

In order to determine if there was a natural frequency around  $2\times$  running speed, a modal impact test was performed while the pumps were not operating. The frequency response spectra are shown in Figures 44 and 45. From these plots, the natural frequencies were detected at 41 Hz and 49.8 Hz similar to those detected from the natural excitation signature plots. Additional natural frequencies were also registered at 59.3 Hz, 60.3 Hz, and 61.6 Hz, which coincides directly with vane pass frequency at  $2\times$  maximum running speed. It is important to mention that the lower modes did become excited when the pump operated at lower speeds, but the vibration levels were significantly lower.

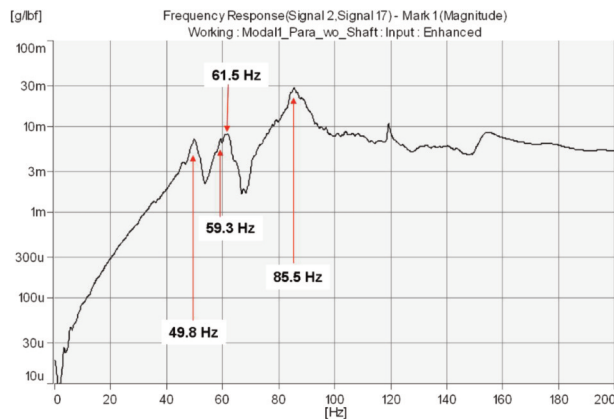


Figure 44. Frequency Response Spectrum from EMA Testing While the Pump Was Not Operating Measured at the Top of the Bearing Housing in the Parallel Direction to the Discharge Piping.

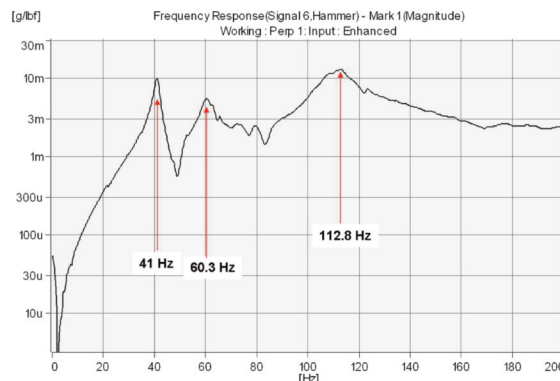


Figure 45. Frequency Response Spectrum from EMA Testing While the Pump Was Not Operating Measured at the Top of the Bearing Housing in the Perpendicular Direction to the Discharge Piping.

The mode shapes at these frequencies were determined from the animations of the ODS models. At 40.0 Hz the entire pump structure was rocking side to side perpendicular to the discharge pipe, as shown in Figure 46. The next main structural natural frequency was identified at 47.4 Hz, which represents the global rocking mode in the parallel direction to the discharge pipe as shown in Figure 47. As can be seen, there is a slight drop in both frequencies when the pump is operating due to minor changes that occur between connecting parts (separation between the pedestal and the foundation or between the pump volute and the pedestal). ODS animation at  $2\times$  rpm indicated excessive flexibility at the bearing tower mounting bracket as shown in Figure 48.

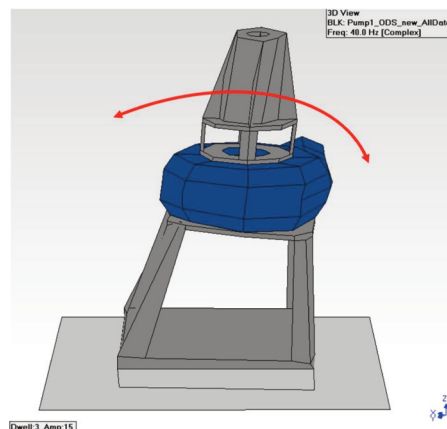


Figure 46. ODS at 40 Hz Natural Frequency of the Pump Showing the Rocking Mode in the Perpendicular Direction.

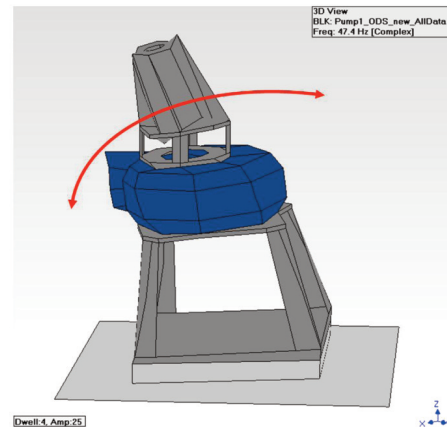


Figure 47. ODS at 47.4 Hz Natural Frequency of the Pump Showing the Rocking Mode in the Parallel Direction.

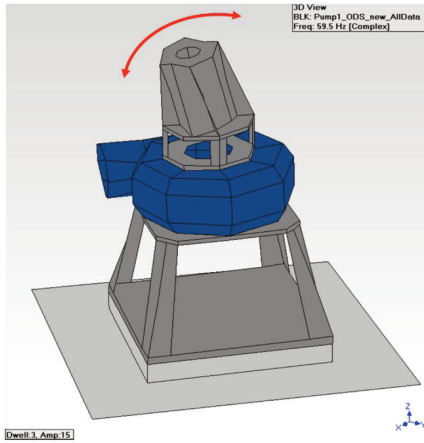


Figure 48. ODS at 2× RPM of the Pump Showing the Excessive Flexibility at the Bearing Tower Mounting Bracket.

Once the offending natural frequencies of the pump structure were identified, the next step was to determine a solution to address not only the bearing tower mode at approximately 60 Hz, but also the two structural rocking modes at 40 Hz and 47.4 Hz that would still become excited at lower speeds in the operating range. At this point in time, it was not clear if the 60 Hz mode was simply a bearing tower structural mode or a more complex pump shaft lateral mode. Rather than implementing a trial and error method to shift all of these natural frequencies outside the 2× running speed range, a detailed FEA model of the pump and drive shaft was created and calibrated to match these frequencies.

#### FEA Analysis and Results

The FEA model of the pump assembly including the suction and discharge piping as well as the drive shaft is shown in Figure 49. Detailed solids models of all the pump components were created from 2D drawings supplied by the pump manufacturer. The pump casing density was adjusted to account for the added mass effect due to the entrapped water in the casing as well as added water mass effects for the impeller. In order to achieve a good correlation of the natural frequencies to the field test data, the pump pedestal had to be constrained at the bolt holes rather than along the entire mounting frame, indicating that the pump was not properly grouted.

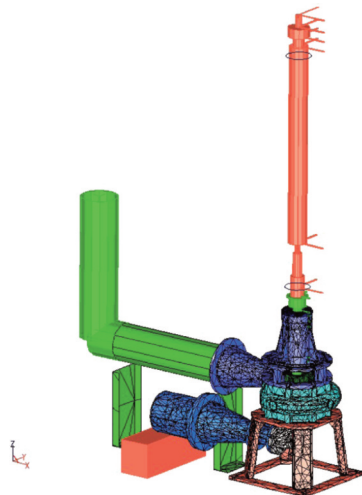


Figure 49. FEA Model for the Pump Assembly with the Suction and Discharge Piping, and the Drive Shaft.

Figure 50 shows the mode shape of the pump predicted at 40 Hz with the same horizontal rocking motion in the perpendicular direction to the discharge pipe that was demonstrated by the ODS

animation. Similarly, Figure 51 shows the mode shape of the pump predicted at 47.8 Hz with the rocking motion in the parallel direction to the discharge pipe.

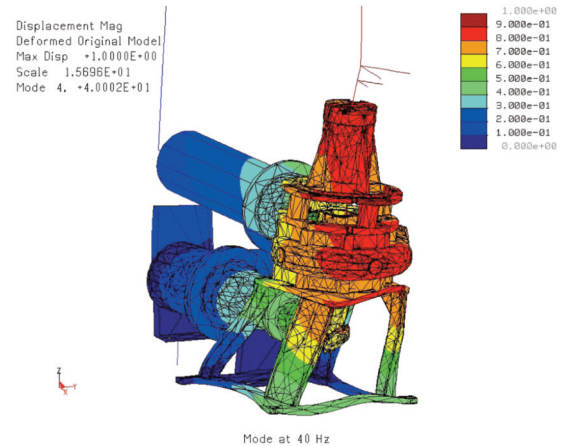


Figure 50. FEA Result Showing Horizontal Rocking Mode at 40 Hz in the Perpendicular Direction.

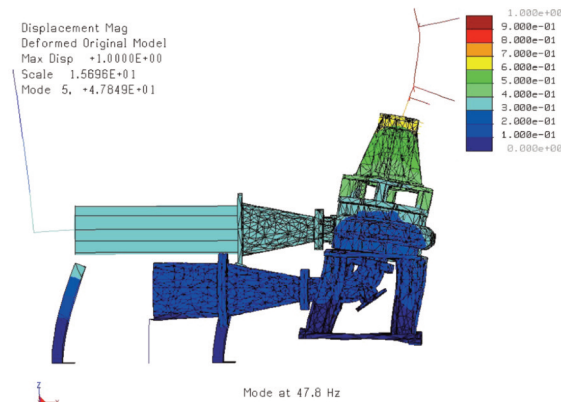


Figure 51. FEA Result Showing Horizontal Rocking Mode at 47.8 Hz in the Parallel Direction.

Figures 52 and 53 show plots of the mode shapes at 59 Hz and 61 Hz, which clearly represent the pump shaft lateral modes in the perpendicular and parallel direction, respectively. The bearing tower also shows some deflection as captured in the ODS, but the majority of the motion takes place at the impeller.

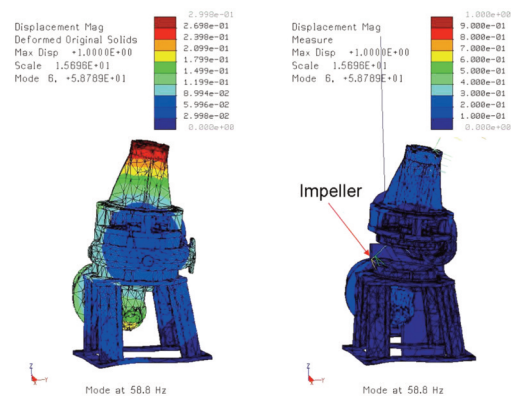


Figure 52. FEA Result Showing the Rotor Lateral Mode at 59 Hz in the Perpendicular Direction. The Contour Plot on the Left Shows the Pump Structure without the Shaft Displayed. The Bearing Tower Moves as Shown in the ODS. The Contour Plot on the Right Shows the Pump without the Casing to Help Visualize the Shaft Mode Where the Majority of the Motion Is Taking Place.

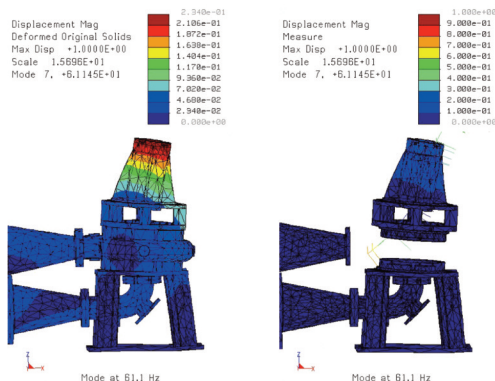


Figure 53. FEA Result Showing the Rotor Lateral Mode at 61.1 Hz in the Parallel Direction. The Contour Plot on the Left Shows the Pump Structure without the Shaft Displayed. The Bearing Tower Moves as Shown in the ODS. The Contour Plot on the Right Shows the Pump without the Casing to Help Visualize the Shaft Mode Where the Majority of the Motion Is Taking Place.

With the FEA model matching the field test data quite accurately, potential fixes were evaluated using the FEA model. While braces could address the structural rocking modes of the pump assembly at 40 Hz and 47.4 Hz, the pump shaft lateral modes would not be significantly affected by these braces and would require changes to the shafting geometry. The FEA demonstrated that this was the case. In order to shift the structural natural frequencies beyond  $2\times$  rpm excitation source, the lowest natural frequency (40 Hz) should be located at least 10 percent above 60 Hz (maximum  $2\times$  rpm), which represents approximately a 65 percent increase in frequency, requiring nearly a threefold increase in stiffness. The mode at 47.4 Hz would also be shifted similarly. Since a large increase in stiffness was required, this was not going to be obtained by simple structural modifications to the pump. Therefore, it was decided that large external braces running from the base of the bearing tower to the concrete foundation would be needed to shift the offending natural frequencies higher. In addition, the pump pedestal was also modified by adding cross-braces between the accessible legs. Since the base of the pedestal structure was not behaving as fully-grouted as intended, it was further recommended that an additional four anchor bolts be installed midspan between the existing corner hold down bolts and the pedestal be regouted. Figure 54 shows the solids model of the proposed bracing modification.

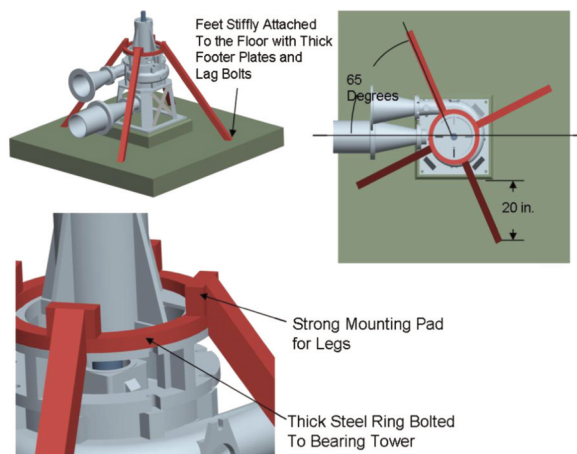


Figure 54. Solids Model of the Pump Assembly Showing the External Braces.

In order to address the pump shaft lateral mode at approximately 60 Hz, attempts were made to stiffen the bearing tower locally with struts, but the analysis showed that this was ineffective. It was clear

that to raise the natural frequency of the rotor mode, the shaft diameter between the bearings would have to be increased. In addition, the upper pump bearing was replaced with a bearing that had a substantial increase in radial stiffness. Considerations were also given to changing the material of the bearing tower from cast-iron to steel to gain approximately twice the stiffness, but the time required to accomplish this made it prohibitive. Based on the analysis results with these modifications, no structural modes were obtained below 100 Hz, which is well beyond the maximum  $2\times$  rpm excitation (60 Hz). Figure 55 shows the FEA results of the rotor lateral modes shifting to 65.4 Hz and 69.5 Hz in the perpendicular and parallel directions, respectively. Originally these frequencies were computed to be a few percent higher due to the fact that the base of the pedestal was to be fully grouted as was expected, and as a result, would be fully constrained, rather than just held at the bolt holes only. Unfortunately, after implementing all the modifications, the base of the pedestal was not regouted, so the above-mentioned frequency numbers were rerun, and they represent the results of the actual installed case, which did not achieve the full 10 percent separation margin that was sought. Figure 56 shows a photo of the final arrangement of the pump after implementing the modifications.

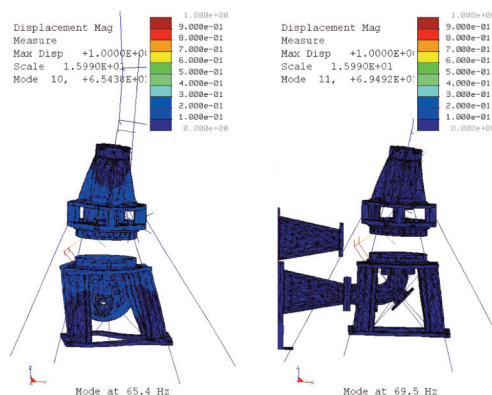


Figure 55. FEA Result after Modifications Showing the Rotor Lateral Mode at 65.4 Hz and 69.5 Hz in the Perpendicular and Parallel Directions, Respectively.



Figure 56. Photo of the Pump Assembly with the Braces.

Follow up test data revealed that the vibration at the running speed (measured at the top of the bearing tower) was reduced 2.5 times to 0.04 in/s (1.02 mm/s) peak, and at  $2\times$  rpm, the vibration



amplitude was reduced 5.8 times to 0.3 in/s (7.62 mm/s) peak. Figures 57 and 58 show the FFT spectra measured at the top of the bearing housing in the perpendicular and parallel direction, respectively. It is clear that the shaft modes shifted up to 64.3 and 66.3 Hz very close to the frequencies predicted by the FEA analysis. Finally, a modal impact test shown in Figure 59 indicated that no natural frequencies were within the  $2\times$  running speed range, and the rotor mode had moved up to 66.5 Hz. It is important to mention that a pronounced natural frequency was present at 50 Hz, which was later determined to be a discharge pipe mode downstream from the check valve.

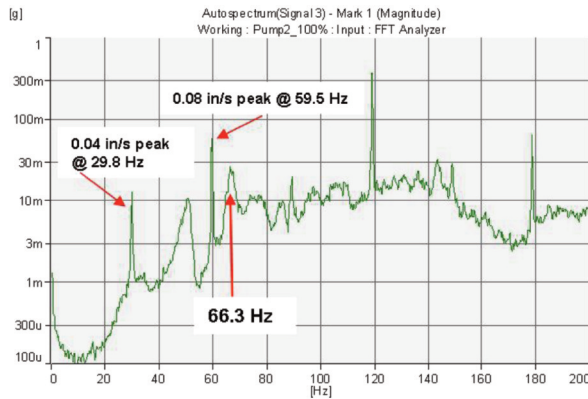


Figure 57. Vibration Spectrum (FFT) Measured at the Top of the Bearing Tower in the Perpendicular Direction to the Discharge Piping after Modifications.

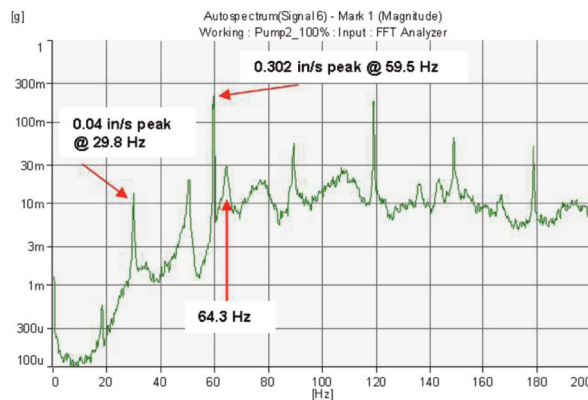


Figure 58. Vibration Spectrum (FFT) Measured at the Top of the Bearing Tower in the Parallel Direction to the Discharge Piping after Modifications.

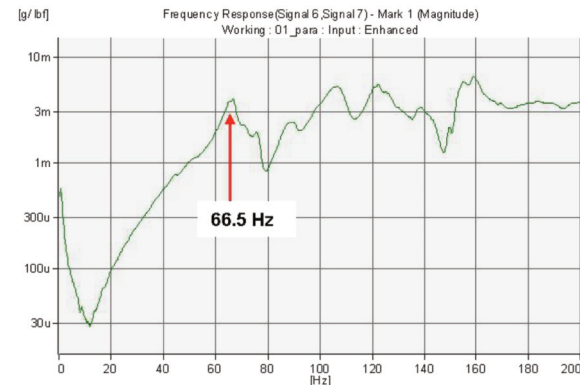


Figure 59. Frequency Response Spectrum from EMA Testing after Modifications While the Pump Was Not Operating Measured at the Top of the Bearing Housing in the Parallel Direction to the Discharge Piping.

### Conclusions and Recommendations

- There were several natural frequencies of the pump structure that fell within the  $2\times$  running speed range, which were being excited by vane pass frequency pressure pulsations. In addition, a pump shaft lateral mode coincided with the maximum  $2\times$  rpm at approximately 60 Hz, which resulted in much higher vibration response than the structural resonances.
- The combination of the field testing (ODS and EMA) and the FEA were able to uncover the root cause of the resonance condition and allowed for virtual fixes to be evaluated with the FEA model prior to actual installation.
- While the external modifications to the pump support and bearing tower would have shifted the structural natural frequencies outside the  $2\times$  running speed range, they would not have provided enough stiffness change to affect the pump shaft lateral modes. Only the FEA analysis allowed for shaft geometry changes and bearing stiffnesses to be evaluated, which provided enough confidence that the internal geometry changes would achieve the desired results.

### CONCLUSIONS

- The ODS is a powerful troubleshooting tool to facilitate and visually understand most vibration problems in any type of turbomachine. Animations created from the ODS test data show exaggerated motion (but consistently scaled) of operating machinery at any given frequency. In most of the cases, the ODS analysis provides enough diagnostic information to identify and solve the problem. Combined with modal “bump” testing during operation, ODS becomes even more powerful.
- Detailed vibration data should be taken when performing an ODS, capturing all flange-to-flange interface areas between assembly parts, flexible components, supports, concrete foundation, etc., as well as the pump casing itself.
- Testing combined with FEA analysis results is an excellent toolset, particularly valuable when good engineering judgment and experience alone have not been successful in diagnosing and fixing vibration problems in centrifugal pumps and other types of turbomachinery.
- Typical vibration field analysis as applied to pursuing trial and error correction methods can be time consuming, cumulatively costly, and will not always achieve the long-term trouble-free operation that is sought. The ODS and FEA toolset, when properly exercised, has an outstanding track record of resulting in rapid problem diagnosis and solution.

### BIBLIOGRAPHY

- Adams, M. L., 2001, *Rotating Machinery Vibration*, New York, New York: Marcel Dekker, Inc.
- Au-yang, M. K., 1937, *Flow-Induced Vibration of Power and Process Plant Components: A Practical Workbook*, Reprint Edition 2001, New York, New York: ASME Press.
- Boyardjis, P. A., 2004, June, “Detecting a Hidden Lateral Rotor Natural Frequency in a Sewage Pump,” *Pumps and Systems Magazine*, pp. 38-45.
- Bowman, D. G., Marscher, W. D., and Reid, S. R., 1990, “Pump Rotor Critical Speeds Diagnosis and Solutions,” *Proceedings of the Seventh International Pump Users Symposium*, Turbomachinery Laboratory, Texas A&M University, College Station, Texas, pp. 73-80.
- Blevins, Robert D., 1979, *Formulas for Natural Frequency and Mode Shape*, Reprint Edition 2001, New York, New York: Van Nostrand Reinhold Company, Inc.

- De Silva, C. W., 2000, *Vibration: Fundamentals and Practice*, Boca Raton, Florida: CRC Press LLC.
- Ewins, D. J. 1984, *Modal Testing: Theory and Practice*, Taunton, Somerset, England: Research Studies Press Ltd.
- Jen, C-W. and Marscher, W. D., 1990, "Experimental Modal Analysis of Turbomachinery Rotors Using Time-Averaging," Proceedings International Modal Analysis Conference, Orlando, Florida.
- McMillan, R. B., 2004, *Rotating Machinery: Practical Solutions to Unbalance and Misalignment*, Lilburn, Georgia: Fairmont Press, Inc.
- Lienau, W. and Lagas, N., 2008, "Evaluation of Rotordynamic Criteria for Multistage Pump Shafts," *Proceedings of the Twenty-Fourth International Pump Users Symposium*, Turbomachinery Laboratory, Texas A&M University, College Station, Texas, pp. 35-44.
- Marscher, W. D., 1986, "Determination of Pump Rotor Critical Speeds During Operation Through Use of Modal Analysis," Proceedings of ASME WAM Symposium on Troubleshooting Methods and Technology, Anaheim, California.
- Marscher, W. D., 1989, "Analysis and Test of Multistage Pump Wet Critical Speeds," ASLE/ASME Joint Tribology Conference, Ft. Lauderdale, Florida.
- Marscher, W. D., 1991, "How to Use Impact Testing to Solve Pump Vibration Problems," Proceedings EPRI Power Plant Pumps Symposium, Tampa, Florida.
- Marscher, W. D., 1997, "Rotating Machinery Vibration and Condition Monitoring," Chapter of *Tribology Data Handbook*, Boca Raton, Florida: CRC Press, pp. 944-955.
- Marscher, W. D., 1999, "The Determination of Rotor Critical Speeds While Machinery Remains Operating through Use of Impact Testing," IMAC Conference, Orlando, Florida.
- Marscher, W. D. and Jen, C-W, 1990, "Using Time-Averaged Modal Excitation to Determine the Rotor Dynamic Bearing Coefficients of Centrifugal Pumps," Proceedings 8th International Modal Analysis Conference, Kissimmee, Florida.
- Marscher, W. D., Boyadjis, P. A., Onari, M. M., Cronin, R. J., Kelly, W. J., Olson, E. J., and Gaydon, M. A., 2008, "Centrifugal Pump Mechanical Behavior and Vibration," Chapter of *Pump Handbook*, Fourth Edition, I. Karassik, J. Messina, P. Cooper, and C. Heald, Editors, New York, New York: McGraw-Hill.
- McConnell, K. G., 1995, *Vibration Testing Theory and Practice*, New York, New York: John Wiley & Sons, Inc.
- Onari, M. M and Gaydon, M. A., 2007, "Solving Vertical Pump Synchronous and Subsynchronous Vibration Problems," Case Studies of the Twenty-Third International Pump Users Symposium, Turbomachinery Laboratory, Texas A&M University.
- Onari, M. M. and Hurrell, C. C., 2008, January/February, "Vibration Failure," *Turbomachinery International Magazine*, 49, (1), pp. 40-42.
- Olson, E. J. and Onari, M. M., 2008, "Solving Structural Vibration Problems Using Operating Deflection Shape (ODS) Analysis," Case Studies of the Thirty-Seventh Turbomachinery Symposium, Turbomachinery Laboratory, Texas A&M University.
- Stavale, A. E., 2008, "Reducing Reliability Incidents and Improving Meantime Between Repair," *Proceedings of the Twenty-Fourth International Pump Users Symposium*, Turbomachinery Laboratory, Texas A&M University, College Station, Texas, pp. 1-10.
- Thomson, W. T. and Dahleh, M. D., 1993, *Theory of Vibration with Applications*, Fifth Edition, Upper Saddle River, New Jersey: Prentice-Hall, Inc.